Structure of Actin Cross-Linked with α-Actinin: A Network of Bundles

O. Pelletier, E. Pokidysheva, L. S. Hirst, N. Bouxsein, Y. Li, and C. R. Safinya*

Materials Department, Physics Department, Biomolecular Science and Engineering Program, University of California, Santa Barbara, California 93106, USA

(Received 15 April 2003; published 30 September 2003)

Three-dimensional laser scanning confocal microscopy has revealed that filamentous actin, when complexed with the cross-linking protein α-actinin, will spontaneously assemble on a micron scale into a structure comprised of a relatively rigid, frequently branching, 3D network of bundles with characteristic mesh size of the order of the persistence length of F-actin. In contrast, additional nanoscale ordering is observed, as synchrotron x-ray diffraction has revealed a disordered, distorted square lattice of actin fibers within the individual bundles.

DOI: 10.1103/PhysRevLett.91.148102 PACS numbers: 87.16.Ka, 61.10.Eq, 61.30.Eb, 61.30.St

Globular (G) actin is among the most abundant proteins in the eukaryotic cell cytoskeleton and the major protein, together with myosin, found in muscle cells. In the presence of ions, G-actin assembles into filamentous (F) actin. Current textbooks on molecular cell biology describe two types of supramolecular assemblies of F-actin [1]. In one type, parallel F-actin rods are assembled into bundles in the presence of bundling proteins, which belong to a large family of actin-binding proteins. In a second type, F-actin rods cross each other at an angle and form, in the presence of specific cross-linking proteins, a network of single filaments. Bundles and networks of actin rods are assembled for a variety of cellular activities; F-actin networks are involved in cell shape, motility, and adhesion. In the fundamental biological process of cell division, leading to growth, F-actin bundles, myosin II motors, and associated biomolecules form a contractile ring, which splits cells into two during cytokinesis.

In our work we studied mixtures of F-actin with the bundling protein α-actinin (from rabbit skeletal muscle, Cytoskeleton, Inc.). α-actinin forms a dimer with the monomers arranged in an antiparallel manner to form a rod-shaped molecule, with an actin-binding region at each end. The molecule has been characterized by electron microscopy as having a width of 3–4 nm and a typical length of $\sim$30 nm [2]. In the cell α-actinin is found in many structures including thick actin bundles known as stress fibers which traverse the cell and lead to adhesion of cells to the extracellular matrix.

In this Letter we describe a new type of supramolecular assembly of F-actin rods and α-actinin into a network of bundles, observed via small angle x-ray scattering (SAXS) and laser scanning confocal microscopy (LSCM). This is the first entirely new type of protein-based supramolecular assembly of F-actin since the bundled and network phases of single filaments were described many years ago. It is extremely important to elucidate the structures of actin solutions on which mechanical and rheological properties of cells are ultimately dependent [2–4].

To prepare α-actinin/actin samples for x-ray scattering, polymerization was carried out at a G-actin concentration of 2 mg/ml. The lyophilized G-actin [5] was first resuspended in a standard buffer solution [6]. Polymerization was initiated by 100 nM KCl and actin filament length controlled by the addition of an appropriate amount of 1 mg/ml gelsolin [7]. For x-ray experiments an actin filament length of 300 nm was preferred as this length minimized the effects of filament fluctuation [8]. The polymerization process was completed after 2 h and phalloidin was added in a 1:1 M ratio with G-actin to stabilize the filaments. The F-actin solution was ultracentrifuged at 50 000 rpm for 2 h at 24 °C using a 100.3 rotor. All supernatant was removed from the sample and the pelleted actin resuspended at 200 mM KCl solution to achieve twice the final KCl concentration with a simultaneous actin concentration of 5 mg/ml. α-actinin [9] solution in buffer was then combined in equal part with the prepared actin (usually 20 μl of each solution) to give 2.5 mg/ml actin samples with the desired α-actinin to G-actin molar ratio (γ). After careful investigation it was found that mixing of the two components was excellent regardless of the method used, therefore a gentle shaking was employed to mix the samples while avoiding actin filament breakage. For a γ ratio greater than 1:100, phase separation occurred within a few hours and a transparent, birefringent, and rather solid pellet was formed. It was found that 15 min of centrifugation on a table centrifuge at 5000 rpm assisted phase separation; therefore all samples were subject to this treatment. The pellets were transferred into 1 mm diameter quartz capillaries for x-ray scattering experiments and sealed to prevent dehydration. X-ray diffraction experiments were carried out at the Stanford Synchrotron Radiation Laboratory at 8 KeV. Data collection was performed on both the beam line 4-2 using a FUJI-BAS image plate and on the 10-2 using a MAR-IMAGE detector.

To prepare samples suitable for LSCM, polymerization of G-actin was carried out as described above. Alexa-Fluor 488 Phalloidin [10] was added to give a 1:1 M ratio of fluorescent dye to G-actin. A drop of α-actinin solution

at 0.3 mg/ml was added to the 0.03 mg/ml F-actin solution directly on a microscope slide. The ionic strength was also adjusted to 200 mM KCl to give a final volume of about 3 μl. The samples were sealed with a cover slip and wax.

LSCM measurements were carried out using a Leica DM IRBE inverted microscope equipped with a Leica confocal system [11]. The excitation wavelength was 488 nm with an emission maximum at 517 nm. A typical acquisition sequence comprised 20 vertical (Z) steps with a resolution of 0.75 μm, at the highest magnification used, the resolution in the XY plane was 0.2 μm per pixel [12]. Confocal microscopy was used to investigate α-actinin/actin bundling on a micron scale. Figure 1 shows images of a sample at $\gamma = 1{:}25$ and 0.01 mg/ml actin concentration. α-actinin has previously been shown to bundle actin filaments [2] and from the figure bundles is immediately apparent. Free actin filaments undergo changes of shape on the scale of seconds, fluctuating freely in solution. In the presence of α-actinin, the threadlike structures observed are less mobile and appear much thicker than single filaments. One of the most interesting features of this system is the formation of an isotropic, networklike structure with a well-defined mesh size. The larger scale image in Fig. 1(a) clearly shows connections between bundles. The LSCM image shows a network mesh size of $\sim$5 μm. This mesh size is of the order of the persistence length of a free actin filament and could possibly be tuned either by changing the actin concentration or by adjusting γ.

Other bundled states of F-actin were compared to the α-actinin system, i.e., bundling by relatively simple counterion condensation [13]. Bundling agents such as $MgCl_2$, $CaCl_2$, and oligolysines were examined and well-defined bundles were formed as expected [14]. Figure 1(b) shows an example of these bundles; few possible connections are evident and a quite different bulk structure is seen with no characteristic mesh size. The Mg^{2+} induced bundles shown are also longer and thicker than their α-actinin induced counterparts with few branching sites. The open network feature of the α-actinin system may be especially important with respect to the biological role of α-actinin within the cell. An interconnected network of bundles induced by the biologically relevant protein α-actinin [Fig. 1(a)] has potentially very different mechanical properties from a system of entangled bundles induced by simple counterions [Fig. 1(b)]. The α-actinin induced network should be expected to provide a much more rigid structure on a micron scale than the non-cross-linked Mg^{2+} structure.

Figure 2 is a three-dimensional image created with confocal software [11] and, using color glasses, one can follow the branching connections between bundles (online only). Conclusive evidence for branching can be found from an analysis of the fluorescence intensity distribution in Fig. 2. For example, two bundles may appear to branch; however, if the bundles are merely crossing

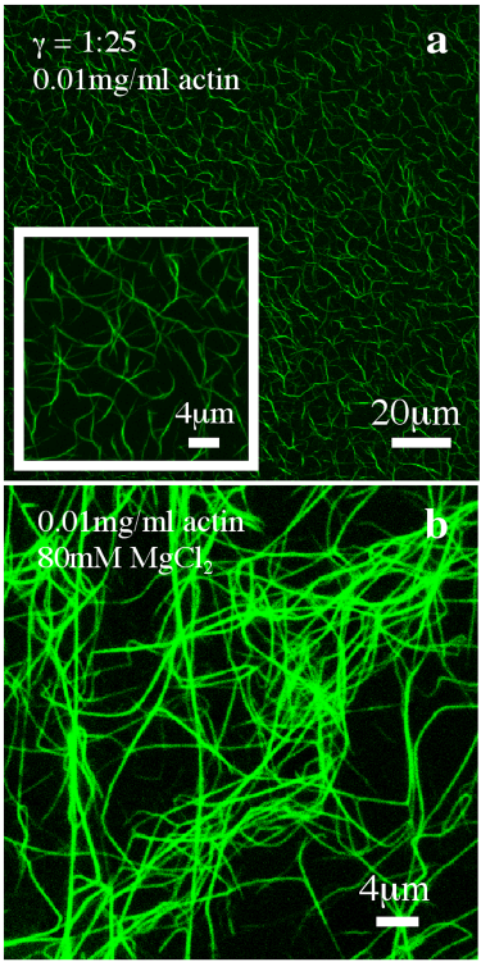

FIG. 1 (color online). LSCM images of (a) α-actinin induced network of actin bundles and (b) counterion (80 mM $MgCl_2$ induced actin bundles.

over, then the fluorescence intensity at the point of intersection should be approximately doubled. In contrast, if a feature is an actual bifurcation, then the fluorescence intensity will be constant across the junction. The crossing sites in 2(b) and (d) demonstrate the increased intensity associated with this kind of junction, whereas 2(a) and (c) show no change in fluorescence intensity across the junction. This figure unambiguously differentiates between the two kinds of intersection and shows clear evidence for branching. This analysis provides further evidence for a 3D network structure on the micron scale and Figs. 1(a) and 2 show a high percentage of branching junctions. Such filament configurations are statistically very unlikely to occur to such a degree unless they correspond to actual connections in the network.

In order to understand the interaction between actin and α-actinin which leads to this previously overlooked self-assembling system, SAXS experiments have been performed to probe the local structural organization within the bundles. Figure 3(a) shows the powder pattern scattering intensity integrated over 360° as a function of q (the scattering vector) for different α-actinin/actin molar

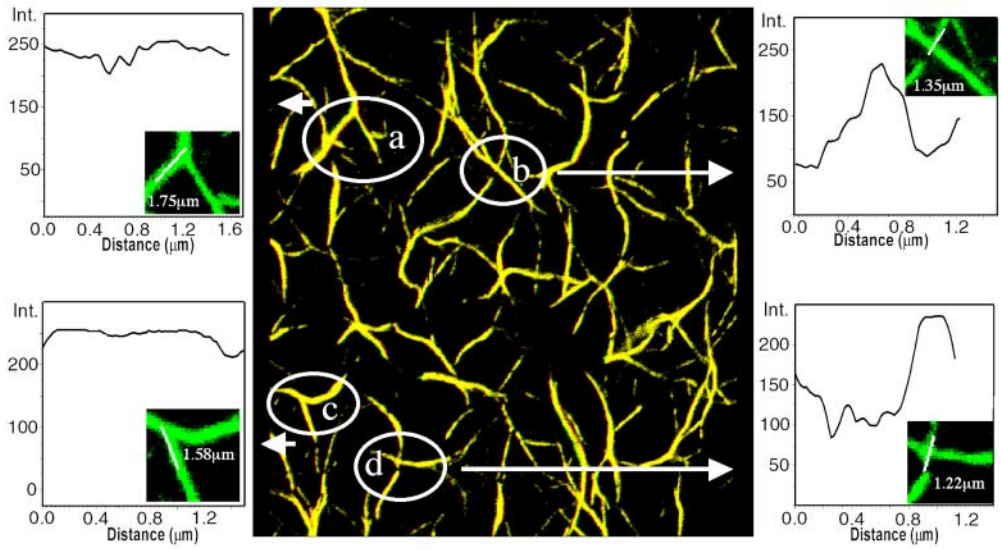

FIG. 2 (color online). A three-dimensional LSCM image of a network of actin bundles at $\gamma = 1{:}5$ with four sites of interest indicated. Ovals (*a*) and (*c*) mark branching sites and (*b*) and (*d*) crossing points. Each indicated area is shown with a fluorescence intensity line profile plot as marked on the inset images.

ratios (γ) at 100 mM KCl concentration and an actin concentration of 2.5 mg/ml. At $\gamma = 1{:}90$ the x-ray diffraction signature is barely different from background, then at $\gamma = 1{:}50$ a sharp increase in small angle scattering is observed. The enhanced SAXS for $\gamma = 1{:}50$ and 1:25 is indicative of the formation of a loose network of F-actin filaments, but where the F-actin–F-actin correlations (observed for $\gamma \leq 1{:}10$) have not yet set in due to the low α-actinin concentration. At $\gamma = 1{:}10$ and above two peaks are visible, and Fig. 3(b) shows a close-up of these features, where peaks can clearly been seen at $q_1 = 0.19\ \mathrm{nm}^{-1}$ and $q_2 = 0.29\ \mathrm{nm}^{-1}$. These results are in good agreement with Tempel *et al.* [4], in which they observe a single fiber network at low γ and bundles at higher γ. The precise peak positions were determined by fitting a $1/q$ background subtraction (scattering from a rod), to the $\gamma = 1{:}5$ sample, then using a fit of two Gaussians [Fig. 3(c)]. The two peaks observed correspond to fiber spacings present inside the bundle and reveal a disordered, distorted square lattice. A perfect hexagonal symmetry for the bundles would give a second order diffraction peak, $q_2 = q_1\sqrt{3} = 0.33$, whereas a perfect square lattice would give $q_2 = q_1\sqrt{2} = 0.27$. The observed second order diffraction peak at $q_2 = 0.29$ is closer to the perfect square position. The 33 nm lattice spacing corresponding to the $q_1 = 0.19\ \mathrm{nm}^{-1}$ peak is approximately equal to the length of the α-actinin molecule and represents strong evidence for a ladderlike bundle structure. This is consistent with previous electron microscopy images, where α-actinin molecules have typically been observed at $\sim 90°$ to the actin filaments [15]. These data, however, reveal for the first time that the actin filaments are organized into a finite-sized distorted square lattice within the bundles. The widths of the two diffraction peaks were measured as 0.056 and $0.136\ \mathrm{nm}^{-1}$, respectively, for $\gamma = 1{:}5$. Inherent disorder leads to diffraction peaks whose widths broaden as q increases and scale as q^2 consistent with our measurements. The peak widths are relatively broad and suggest a domain size of ~ 50 nm compared with the observed bundle diameter of ~ 400 nm, indicating an extremely disordered lattice within the bundle. Figure 4

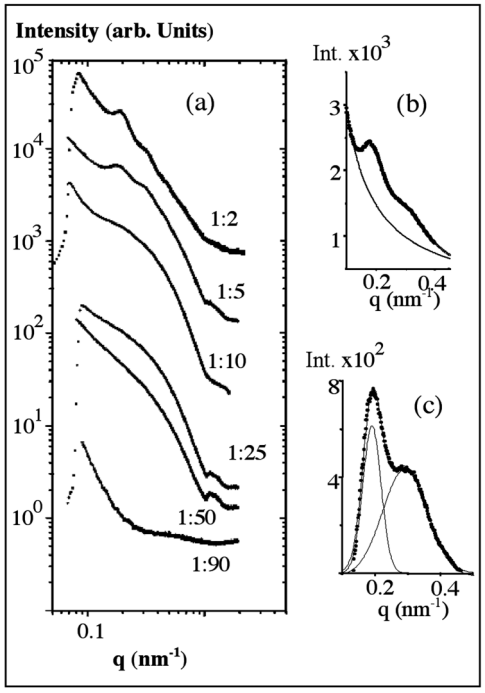

FIG. 3. SAXS scattering intensity as a function of q for (a) several different values of γ, (b) in detail for $\gamma = 1{:}5$ shown with a $1/q$ background fit, and (c) $\gamma = 1{:}5$ data with background subtraction and Gaussian fits to the peaks at $q = 0.19$ and $0.29\ \mathrm{nm}^{-1}$.

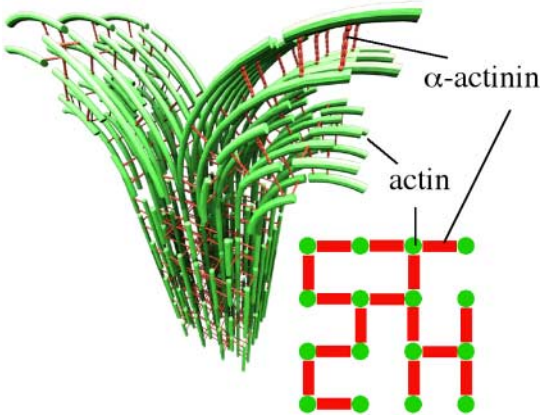

FIG. 4 (color online). Cartoon showing the proposed structure of an F-actin bundle at a branching site, where F-actin is cross-linked with α-actinin. A cross sectional projection of the bundle is also shown. The broad x-ray peaks observed for such bundles indicate a disordered lattice with distorted square symmetry as described in the text.

demonstrates the ladderlike structure within the bundles at a branching site. It is proposed that the bundling process proceeds in a zipperlike fashion between adjacent fibers. At a bifurcation point an F-actin fiber will bend away from the main bundle where new fibers zip on creating a branch.

Having revealed the F-actin lattice spacing it is clear that the elastic properties of the bundled actin phase vary greatly on different length scales. On a micron scale we observe a fairly rigid, 3D network structure in the α-actinin/actin system in contrast to the flexible bulk characteristics of a counterion bundled phase. On a nanometer length scale there are also marked differences. The widely spaced lattice observed within the α-actinin/actin bundle is fairly porous and expected to be highly compressible in contrast to the tightly packed counterion induced bundles [14]. The SAXS peak positions do not change as a function of γ; however, in this study we observe peaks only at $\gamma = 1{:}10$ and above. Over the investigated actin concentration range from 0.02 to 1.5 mg/ml, the peak positions remain constant. The gradual disappearance of the bundling peaks with increasing peak width as γ decreases is not reflected in LSCM studies of the same system. In fact, at low γ, bundles can be observed optically [i.e., at 1:25 in Fig. 1(a)] but the x-ray peaks cannot be resolved at this ratio. The broadening of the peak widths with decreasing γ ratio, with peak positions remaining constant, can therefore be interpreted as an increase in the disorder of the system, due to the reduced number of α-actinin linkers per unit length of actin filament (cross section in Fig. 4), and not as a gradual transition towards another kind of local order.

In this Letter the macromolecular structures of α-actinin induced F-actin bundles have been investigated on both the micron and nanoscales. The α-actinin/actin bundle system has been shown to exhibit a highly branched 3D network structure with a characteristic mesh size. The nanoscale packing structure of F-actin fibers in α-actinin bundles has also been elucidated, revealing a loosely packed, disordered square lattice. This structure is distinct from the close packed structures observed previously in actin bundles in the presence of simple divalent counterions [14]. It is clear from these findings that the structures formed by the α-actinin bundle system are of considerable interest. The physical properties of this system are both unusual and fascinating, with broad potential applications in the field of nanotechnology. A more detailed investigation into the role of α-actinin induced actin networks in the cell will no doubt reveal more on the use of this important protein and its role in cell functionality.

It is a pleasure to acknowledge many useful discussions with G. C. L. Wong. This work was supported by NSF Grants No. DMR-0203755, No. CTS-0103516 (NIRT), and No. DMR-0080034 (UCSB MRSEC), NIH Grant No. GM-59288, and the Department of Energy's Office of Basic Energy Sciences under Contract No. W-7405-ENG-34 with the University of California.

*Corresponding author.
Email address: safinya@mrl.ucsb.edu

[1] H. Lodish *et al.*, *Molecular Cell Biology* (Freeman, San Francisco, 1999), 4th ed.
[2] M. Imamura, T. Endo, M. Kuroda, T. Tanaka, and T. Masaki, J. Biol. Chem. **263**, 7800 (1988); K. A. Taylor and D. W. Taylor, Biophys. J. **67**, 1976 (1994).
[3] P. A. Janmey, S. Hvidt, J. Kas, D. Lerche, A. Maggs, E. Sackmann, M. Schliwa, and T. P. Stossel, J. Biol. Chem. **269**, 32 503 (1994).
[4] M. Tempel, G. Isenberg, and E. Sackmann, Phys. Rev. E **54**, 1802 (1996).
[5] Purified G-actin, purity $> 95\%$, was purchased from Cytoskeleton, Inc., Denver, CO 80206.
[6] G-actin buffer, 5 mM Tris-HCl, 0.2 mM $CaCl_2$, 0.5 mM ATP, 0.2 mM DTT.
[7] Gelsolin from human plasma in a 150 mM NaCl, 2.7 mM KCl, 8 mM Na_2HPO_4, 1 mM EGTA, *p*H 7.2 buffer was purchased from Cytoskeleton, Inc.
[8] G. C. L. Wong, J. X. Tang, A. Lin, Y. L. Li, P. A. Janmey, and C. R. Safinya, Science **288**, 2035 (2000).
[9] α-actinin from Cytoskeleton, Inc., in a 20 mM NaCl, 20 mM tris-HCl, *p*H 8.0, 5 mM BME, 5% glycerol buffer.
[10] Purchased from Molecular Probes Inc., Eugene, OR.
[11] Leica Microsystems Inc., Exton, PA 19341.
[12] A. J. Lin, N. L. Slack, A. Ahmad, C. X. George, C. E. Samuel, and C. R. Safinya, Biophys. J. **84**, 3307 (2003).
[13] J. X. Tang and P. A. Janmey, J. Biol. Chem. **271**, 8556 (1996).
[14] G. C. L. Wong, A. Lin, J. X. Tang, Y. L. Li, P. A. Janmey, and C. R. Safinya, Phys. Rev. Lett. **91**, 018103 (2003).
[15] R. K. Meyer and U. Aebi, J. Cell Biol. **110**, 2013 (1990).